Broken symmetry and pseudogaps in ropes of carbon nanotubes

Delaney, P., Choi, H. J., Ihm, J., Louie, S. G., & Cohen, M. L. (1998). Broken symmetry and pseudogaps in ropes of carbon nanotubes. Nature, 391(6666), 466-468. DOI: 10.1038/35099

Published in:
Nature

12. Dallesasse, J. M., Holonyak, J. N., Sugg, A. R., Richard, T. A. & El-Zein, N. Hydrolysation oxidation of AlGaAs-AlAs-GaAs quantum well heterostructures and superlattices. *Appl. Phys. Lett.* **57,** 2844–2846 (1990).
13. Huffaker, D. L., Deppe, D. G. & Kumar, K. Native-oxide defined ring contact for low-threshold vertical-cavity lasers. *Appl. Phys. Lett.* **65,** 97–99 (1994).
14. MacDougal, M. H., Zao, H., Dapkus, P. D., Ziari, M. & Steier, W. H. Wide-bandwidth distributed bragg reflectors using oxide/GaAs multilayers. *Electron. Lett.* **30,** 1147–1149 (1994).
15. Fiore, A. *et al.* $\Delta n = 0.22$ birefringence measurement by surface emitting second harmonic generation in selectively oxidized GaAs/AlAs optical waveguides. *Appl. Phys. Lett.* **71,** 2587–2589 (1997).

Acknowledgements. This work was partially supported by the European Community under the IT "OFCORSE" Programme.

Correspondence and requests for materials should be addressed to V.B. (e-mail: berger@thomson-lcr.fr).

Broken symmetry and pseudogaps in ropes of carbon nanotubes

Paul Delaney*, Hyoung Joon Choi*†, Jisoon Ihm*†, Steven G. Louie* & Marvin L. Cohen*

** Department of Physics, University of California at Berkeley, and Materials Sciences Division, Lawrence Berkeley National Laboratory, Berkeley, California 94720, USA*
† Department of Physics and Center for Theoretical Physics, Seoul National University, Seoul 151-742, Korea

Since the discovery of carbon nanotubes[1], it has been speculated that these materials should behave like nanoscale wires with unusual electronic properties and exceptional strength. Recently, 'ropes' of close-packed single-wall nanotubes have been synthesized in high yield[2]. The tubes in these ropes are mainly of the (10,10) type[3], which is predicted to be metallic[4–6]. Experiments on individual nanotubes and ropes[7,8] indicate that these systems indeed have transport properties that qualify them to be viewed as nanoscale quantum wires at low temperature. It has been expected that the close-packing of individual nanotubes into ropes does not change their electronic properties significantly. Here, however, we present first-principles calculations which show that a broken symmetry of the (10,10) tube caused by interactions between tubes in a rope induces a pseudogap of about 0.1 eV at the Fermi level. This pseudogap strongly modifies many of the fundamental electronic properties: we predict a semimetal-like temperature dependence of the electrical conductivity and a finite gap in the infrared absorption spectrum. The existence of both electron and hole charge carriers will lead to qualitatively different thermopower and Hall-effect behaviours from those expected for a normal metal.

Carbon nanotubes are tubular structures which are typically a few nanometres in diameter and many micrometres in length. These quasi-one-dimensional systems are predicted[4–6] to have an electronic structure dictated by their geometric structure. In particular, an isolated armchair-type nanotube (one whose roll-up indices are (n, n)) has two linear bands which cross at the Fermi level. These two linear bands give rise to a constant density of states near the Fermi level and to metallic behaviour in conduction and other physical properties. One of the bands has π-bonding and the other has π-antibonding character. An isolated (n, n) nanotube has n mirror planes containing the tube axis. The π-bonding state is even (the wavefunction has no sign change) and the π-antibonding state is odd (sign change) under these symmetry operations. The band crossing is allowed and the armchair nanotube is metallic as shown schematically in Fig. 1a. It is precisely this symmetry of the isolated (n, n) tube that gives its desired metallic behaviour[9], and this property motivates many of the recent electrical measurements. Breaking of this symmetry, however, will completely alter this picture.

With the rope axis vertical, if one were to separate the tubes in a rope far enough to eliminate any interactions between the tubes, then the energy bands of the rope would have no dispersion in the horizontal plane, and the band structure along any vertical line in reciprocal space would be identical to that of a single isolated tube, with a band crossing as shown in Fig. 1a. However, the actual distances between tubes in the ropes are small enough that each nanotube can feel the potential due to all the other nanotubes. As a result of this perturbation, the Hamiltonian at any point k where the two bands used to cross becomes

$$H_k = \begin{pmatrix} \epsilon_0 + \delta_{11} & \delta_{12} \\ \delta_{21} & \epsilon_0 + \delta_{22} \end{pmatrix} \quad (1)$$

where ϵ_0 is the unperturbed energy. The diagonal matrix elements δ_{11} and δ_{22} merely act to shift the energy and location in k-space of the band crossing. It is the off-diagonal elements that cause quantum-mechanical level repulsion and therefore open a gap as shown schematically in Fig. 1b. If the vertical line through k has high

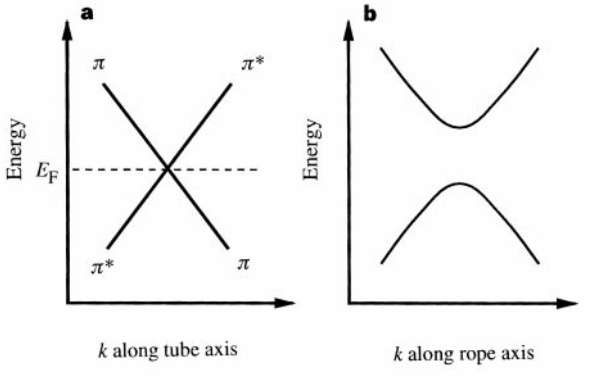

Figure 1 Band crossing and band repulsion. **a**, Schematic diagram of the crossing of two linear bands for an isolated (n,n) carbon nanotube. One band has π-bonding character and the other has π-antibonding (π^*) character. E_F is the Fermi energy and k is the wavevector. **b**, Repulsion of bands due to breaking of mirror symmetry.

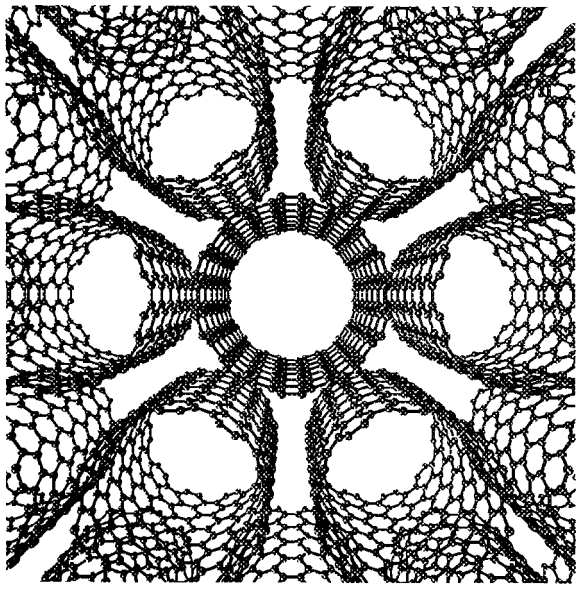

Figure 2 Perspective view of a rope of (10,10) carbon nanotubes. Along the horizontal axis one can see the alignment of the chains of hexagons between neighbouring nanotubes.

symmetry, the off-diagonal matrix elements may still be zero and a crossing may persist. However, at a general k-point the inter-tube interactions, which have not been considered in detail in the past, will dramatically change the physics of the ropes.

To determine the character and magnitude of the pseudogap, we make calculations including the full interaction between the tubes using both the *ab initio* pseudopotential local-density-functional method and the empirical pseudopotential method[10] (EPM). The empirical pseudopotential is generated so as to reproduce the band structure of a single graphene sheet and of graphite[11] accurately near the Fermi level. With this choice, our potential captures both the intra- and inter-tube interactions and describes the electronic structure of the rope correctly. With the EPM, the computational effort is considerably reduced, allowing a detailed investigation of the electronic states of the ropes. Our *ab initio* pseudopotential band structures for the ropes at selected k-points confirm the EPM results.

Experimentally, the ropes are found to contain hundreds of tubes of nearly uniform diameter forming a triangular lattice[3]. In this work, the (10,10) tubes are packed in a hexagonal array in the x–y plane with the tube axes along the z-direction and with the intertube carbon–carbon distance being 3.3 Å. This arrangement is depicted in Fig. 2. The rotational orientation of the tubes relative to each other determines the symmetry of the structure and has an important bearing on the band structure near the Fermi level.

First, we consider the general case where the tubes are rotated by an arbitrary angle (that is misaligned) about the z-axis, so that the rope as a whole loses all vertical mirror planes. The symmetry is low (C_{2h} group) and the off-diagonal matrix element $\delta_{21}(k) = \langle\pi^*|H_k|\pi\rangle \neq 0$ in general. The two bands near the Fermi energy repel, and open a gap as explained above. The rope does not immediately become a semiconductor, however. Because of the periodicity in the x–y plane, different perpendicular components $k_\perp = (k_x, k_y)$ of k-vectors exist in the Brillouin zone and the split bands go up and down by different amounts according to the magnitude of the diagonal matrix elements $\delta_{11}(k) = \langle\pi|H_k|\pi\rangle$ and $\delta_{22}(k) = \langle\pi^*|H_k|\pi^*\rangle$. Bands at different $k_\perp$ tend to overlap, and so even if there is a gap along the k_z-direction for each $k_\perp$, the rope may still be metallic.

To model this general case, we perform a calculation where a vertical row of hexagons in one tube lines up 1.5° off from perfect alignment with a hexagon row in one of the neighbouring tubes. The calculated density of states (DOS) is plotted with a broken line in Fig. 3a. Gaps open in the band structure which create a valley of ~0.1 eV width in the DOS curve. The DOS at the Fermi level is still about 1/3 of the average density of states: this non-zero value is due to the overlap of bands at different $k_\perp$ as expected from the above argument. We call this valley in the DOS at the Fermi level a pseudogap. This is in sharp contrast to the DOS of an isolated tube which is essentially constant within a range of ±1 eV from the Fermi energy.

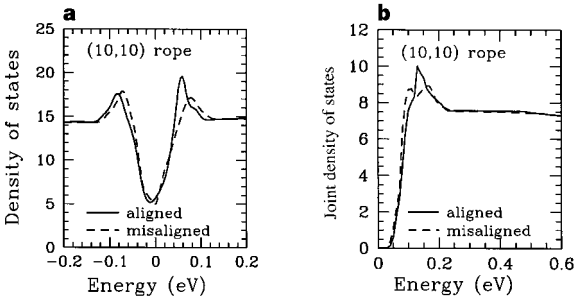

Figure 3 Calculated densities of states. **a**, Calculated density of states for a rope of misaligned (10,10) tubes (broken line) and aligned tubes (solid), in units of states per meV per atom. The Fermi energy is set at zero. **b**, Calculated joint density of states for a rope of misaligned (10,10) tubes (broken line) and aligned tubes (solid), in units of states per meV per atom.

To examine the effect of orientation, we next consider the special case where the tubes are aligned so that a vertical chain of hexagons along one tube lines up exactly with another chain of hexagons on a neighbouring tube. This is the most symmetric situation (D_{2h} group), and some reflection symmetry is preserved. However, unlike the case of the isolated tube, band crossing in the three-dimensional rope requires additional conditions on the electronic states. Our calculations show that the crossing of the two linear bands does occur along particular high-symmetry lines of $k_\perp$ in the Brillouin zone. Previous calculations on a hexagonal lattice of the smaller (6,6) carbon nanotube have shown similar features[12]. At all other values of $k_\perp$, bands again split. The calculated DOS in this case is plotted with a solid line in Fig. 3a. As the measure of the high-symmetry k-points in k-space is zero, there is no significant change in the DOS near the Fermi level. This leads to the important conclusion that the DOS (and hence properties related to it) does not depend on the details of the relative orientations of the tubes. The existence of the pseudogap due to the broken symmetry in the rope makes the conductivity and other transport properties significantly different from those of isolated tubes, even without considering the effect of local disorder in low dimensions[13,14]. The carrier density will increase as the temperature is raised because the DOS increases quickly away from the Fermi level, as shown in Fig. 3a. This structure in the DOS will also make the properties of the rope sensitive to doping.

The π-bonding and π-antibonding states produce two Fermi surfaces. Under the assumption of the highest possible symmetry (D_{2h}) of the rope, we find a pocket of electron-like states in the shape of a rhombic pancake and another pocket of hole-like states in a similar shape. As the periodic structure and the symmetry are disturbed in real ropes, we expect that the Fermi surfaces are smeared out to some degree. A rather complex temperature dependence of thermopower and Hall effects is expected because of the coexistence of electrons and holes as well as the partial smearing out of the Fermi surfaces.

To examine the optical properties, we calculate the joint density of states (JDOS) for both orientations of the tubes in the rope (Fig. 3b). The JDOS is defined by

$$\mathrm{JDOS}(E) = \sum_{o,u} \frac{1}{4\pi^3} \int_{\mathrm{BZ}} \mathrm{d}^3k\,\delta(E_k^u - E_k^o - E) \qquad (2)$$

where o and u run over the occupied and unoccupied states respectively, and BZ is the Brillouin zone. For an isolated tube, because of the two linear bands crossing at the Fermi level, the JDOS has a nonzero value at $E = 0$ and remains almost constant up to ~1 eV. In a rope, on the other hand, the band repulsion makes the JDOS at $E = 0$ vanish completely. The band overlap for different $k_\perp$ does not change the JDOS because the JDOS measures the transition energy for each given (conserved) k-vector, as defined in equation (2). Although the symmetrically aligned tubes do produce band crossings at some high-symmetry k-points, the measure of those k-points contributing to the JDOS at $E = 0$ is again zero, and the misaligned and aligned tubes do not show significant differences in Fig. 3b. Infrared absorption measurements should show the difference in behaviour between the isolated tubes and the rope. However, we wish to note that the vertical (k-conserving) transitions of electronic states assumed in equation (2) may have to be relaxed in the study of ropes. As a real rope does not have a perfectly periodic structure, k-conservation is only approximately valid. In the extreme case of complete disorder, an infrared experiment would reflect the DOS rather than the JDOS. In the present case, an infrared measurement would show features in between the JDOS prediction of a gap of a few tens of meV and the DOS prediction of a pseudogap.

Finally, as a stronger external perturbation in general would lead to a larger band repulsion, a rope could behave like a semiconductor under a sufficiently strong perturbation. This may be an explanation for the quantum dot behaviour of isolated tubes and ropes[7,8] in which some semiconductor barrier region seemingly develops at the contact where a substantial perturbation in potential is expected to occur. □

Received 23 July; accepted 17 November 1997.

1. Iijima, S. Helical microtubules of graphitic carbon. *Nature* **354,** 56–58 (1991).
2. Thess, A. *et al.* Crystalline ropes of metallic carbon nanotubes. *Science* **273,** 483–487 (1996).
3. Cowley, J. M., Nikolaev, P., Thess, A. & Smalley, R. E. Electron nano-diffraction study of carbon single-walled nanotube ropes. *Chem. Phys. Lett.* **265,** 379–384 (1997).
4. Hamada, N., Sawada, S. & Oshiyama, A. New one-dimensional conductors: graphitic microtubules. *Phys. Rev. Lett.* **68,** 1579–1581 (1992).
5. Mintmire, J. W., Dunlap, B. I. & White, C. T. Are fullerene tubules metallic? *Phys. Rev. Lett.* **68,** 631–634 (1992).
6. Saito, R., Fujita, M., Dresselhaus, G. & Dresselhaus, M. S. Electronic structure of chiral graphene tubules. *Appl. Phys. Lett.* **60,** 2204–2206 (1992).
7. Tans, S. J. *et al.* Individual single-wall carbon nanotubes as quantum wires. *Nature* **386,** 474–477 (1997).
8. Bockrath, M. *et al.* Single-electron transport in ropes of carbon nanotubes. *Science* **275,** 1922–1925 (1997).
9. Krotov, Y. A., Lee, D.-H. & Louie, S. G. Low energy properties of (*n*,*n*) nanotubes. *Phys. Rev. Lett.* **78,** 4245–4248 (1997).
10. Cohen, M. L. & Chelikowsky, J. R. *Electronic Structure and Optical Properties of Semi-conductors*, 20 (Springer, Berlin, 1988).
11. Charlier, J.-C., Gonze, X. & Michenaud, J.-P. First-principles study of the stacking effect on the electronic properties of graphites. *Carbon* **32,** 289–299 (1994).
12. Charlier, J.-C., Gonze, X. & Michenaud, J.-P. First-principles study of carbon nanotube solid-state packings. *Europhys. Lett.* **29,** 43–48 (1995).
13. Song, S. N., Wang, X. K., Chang, R. P. H. & Ketterson, J. B. Electronic properties of graphite nanotubules from galvanomagnetic effects. *Phys. Rev. Lett.* **72,** 697–700 (1994).
14. Langer, L. *et al.* Quantum transport in a multiwalled carbon nanotube. *Phys. Rev. Lett.* **76,** 479–482 (1996).

Acknowledgements. We thank V. Crespi for discussions and for providing relaxed atomic coordinates. This work was supported by the NSF and DOE. P.D. thanks the NUI for support; H.J.C. and J.I. were supported by the BSRI program of the Ministry of Education of Korea and the SRC program of KOSEF; and S.G.L. acknowledges the hospitality of the Aspen Center for Physics.

Correspondence should be addressed to S.G.L. (e-mail: louie@jungle.berkeley.edu).

Recognition of the four Watson–Crick base pairs in the DNA minor groove by synthetic ligands

Sarah White, Jason W. Szewczyk, James M. Turner, Eldon E. Baird & Peter B. Dervan

Division of Chemistry and Chemical Engineering and Beckman Institute, California Institute of Technology, Pasadena, California 91125, USA

The design of synthetic ligands that read the information stored in the DNA double helix has been a long-standing goal at the interface of chemistry and biology[1–5]. Cell-permeable small molecules that target predetermined DNA sequences offer a potential approach for the regulation of gene expression[6]. Oligodeoxynucleotides that recognize the major groove of double-helical DNA via triple-helix formation bind to a broad range of sequences with high affinity and specificity[3,4]. Although oligonucleotides and their analogues have been shown to interfere with gene expression[7,8], the triple-helix approach is limited to recognition of purines and suffers from poor cellular uptake. The subsequent development of pairing rules for minor-groove binding polyamides containing pyrrole (Py) and imidazole (Im) amino acids offers a second code to control sequence specificity[9–11]. An Im/Py pair distinguishes G·C from C·G and both of these from A·T/T·A base pairs[9–11]. A Py/Py pair specifies A,T from G,C but does not distinguish A·T from T·A[9–14]. To break this degeneracy, we have added a new aromatic amino acid, 3-hydroxypyrrole (Hp), to the repertoire to test for pairings that discriminate A·T from T·A. We find that replacement of a single hydrogen atom with a hydroxy group in a Hp/Py pairing regulates affinity and specificity by an order of magnitude. By incorporation of this third amino acid, hydroxypyrrole–imidazole–pyrrole polyamides form four ring-pairings (Im/Py, Py/Im, Hp/Py and Py/Hp) which distinguish all four Watson–Crick base pairs in the minor groove of DNA.

Because of the degeneracy of the hydrogen-bond donors and acceptors displayed on the edges of the base pairs, the minor groove was thought to lack sufficient information for a complete recognition code[15]. But, despite the central placement of the guanine exocyclic N2 amine group in the G,C minor groove[15,16], Py/Im and Im/Py pairings distinguish energetically between G·C and C·G[9–11,17,18]. The neighbouring Py packs an Im to one side of the minor groove resulting in a precisely placed hydrogen bond between Im N3 and guanine N2 for specific recognition[19,20]. This remarkable sensitivity to single atomic replacement indicates that substitution at the 3 position of one Py within a Py/Py pair can complement small structural differences at the edges of the base pairs in the centre of the minor groove. For A,T base pairs, the hydrogen-bond acceptors at N3 of adenine and O2 of thymine are almost identically placed in the minor groove, making hydrogen-bond discrimination a challenge (Fig. 1)[15]. The existence of an asymmetrically placed cleft on the minor groove surface between the thymine O2 and the adenine 2H suggests a possible shape-selective mechanism for A·T recognition[21]. We reasoned that substitution of C3–H by C3–OH within a Py/Py pair would create 3-hydroxypyrrole (Hp)/Py pairings to discriminate T·A from A·T (Fig. 2). Selectivity could potentially arise from steric destabilization of polyamide binding via placement of Hp opposite A or stabilization by specific hydrogen bonds between Hp and T.

Four-ring polyamide subunits, covalently coupled to form eight-ring hairpin structures, bind specifically to 6-base-pair (bp) target sequences at subnanomolar concentrations[11,18]. We report here the DNA-binding affinities of three eight-ring hairpin polyamides containing pairings of Im/Py, Py/Im opposite G·C, C·G and either Py/Py, Hp/Py or Py/Hp at a common single point opposite T·A and A·T (Fig. 2b). Equilibrium dissociation constants (K_D) for ImImPyPy-γ-ImPyPyPy-β-Dp (**1**), ImImPyPy-γ-ImHpPyPy-β-Dp (**2**), and ImImHpPy-γ-ImPyPyPy-β-Dp (**3**) were determined by

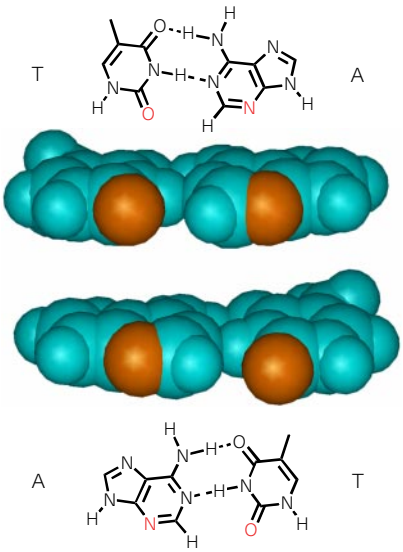

Figure 1 Chemical structures and space-filling models of the T·A and A·T base pairs as viewed from the minor groove of DNA. Models generated using B-form DNA coordinates provided in InsightII. The hydrogen-bond acceptors (N3 of adenine and O2 of thymine) are in red.